Acta Crystallographica Section D
Biological Crystallography
ISSN 0907-4449

Structure of cytochrome c_2 from *Rhodospirillum centenum*

A. Camara-Artigas,† J. C. Williams and J. P. Allen*

Department of Chemistry and Biochemistry, Arizona State University, Tempe, AZ 85287-1604, USA

† Permanent address: Dpto Química Física, Bioquímica y Química Inorgánica, Universidad de Almería, Spain.

Correspondence e-mail: jallen@asu.edu

Received 7 March 2001
Accepted 22 June 2001

PDB Reference: cytochrome c_2, 1jdl.

Cytochrome c_2 from the purple photosynthetic bacterium *Rhodospirillum centenum* has been crystallized by the sitting-drop vapour-diffusion method. The crystals belong to the orthorhombic space group $P2_12_12_1$, with unit-cell parameters a = 29.7, b = 59.9, c = 65.4 Å, and diffract to a resolution limit of 1.7 Å. The Fe-atom position was determined from its anomalous scattering contribution and a molecular-replacement solution was calculated. The correctness of the solution was confirmed by parallel isomorphous replacement studies. The resulting model has a type I cytochrome fold with two features, an extended α-helix and a surface-charge distribution, that are distinctive to this protein. The implications of these structural features for the ability of the cytochrome to serve as an electron carrier are discussed.

1. Introduction

Cytochromes are a general class of water-soluble proteins that serve as electron carriers in many different organisms (Moore & Pettigrew, 1990). In photosynthetic bacteria, cytochrome c_2 functions as a shuttle for electrons between the cytochrome bc_1 complex and the reaction centers (Meyer & Donohue, 1995). In many photosynthetic bacteria, including *R. centenum*, the reaction center contains a tetraheme subunit that serves as the binding site for the cytochrome c_2. In this case, the hemes of the tetraheme subunit serve as intermediate participants in the transfer of electrons from cytochrome c_2 to the photo-oxidized bacteriochlorophyll dimer of the reaction center. In other bacterial systems, such as *Rhodobacter sphaeroides*, the reaction center lacks a tetraheme subunit and the cytochrome c_2 directly transfers an electron to the oxidized dimer.

The electron-transfer domain of cytochromes centers on the solvent-accessible heme edge called the 'frontside' region (Salemme *et al.*, 1973). This 'frontside' region has a significant number of conserved lysine residues that interact electrostatically with carboxylate groups of other proteins to drive the reversible formation of cytochrome–protein complexes. The kinetic behavior of electron transfer to bacterial reaction centers for cytochrome c_2 isolated from *R. centenum* is different to that for cytochrome c_2 from other purple bacteria, owing to the approximate 20-fold decrease in binding affinity (Lin *et al.*, 1994; Wang *et al.*, 1994). Comparison of amino-acid sequences suggests that the decrease in binding relative to other cytochromes may be a consequence of the lower number of lysine residues of this cytochrome c_2 and a related isozyme from *R. centenum* (Samyn *et al.*, 1998). To investigate the structural aspects that give rise to these kinetic differences, we have determined the structure of the cytochrome c_2 from *R. centenum* using X-ray diffraction.

2. Experimental

2.1. Purification of cytochrome c_2

Bacterial cell growth was performed as previously described (Yildiz *et al.*, 1991). After harvesting the cells, the protein was purified as described by Bartsch (1978) with the following modifications. The periplasmic extract was adjusted to 30% saturated ammonium sulfate and placed onto an *n*-butyl Toyopearl column (Toso-Haas). Under these conditions, the cytochrome did not bind and the eluent was collected. The ammonium sulfate concentration of the eluent was increased to 60% saturation and reapplied to the column. The cytochrome c_2 now bound to the column and was washed with a 60% saturated ammonium sulfate solution. After washing, the cytochrome was eluted with a 60–0% saturated ammonium sulfate gradient. The cytochrome was desalted using a Sephadex G-25 column and further purified using a DEAE Toyopearl anion-exchange column (Toso-Haas). After elution using an NaCl gradient, the cytochrome was dialyzed against 10 m*M* phosphate buffer pH 7. Reaction centers from *R. centenum* were prepared as previously described (Wang *et al.*, 1994).

2.2. Protein sequencing

The amino-acid sequence was determined using automated Edman degradation (Porton 2090E). The N-terminal amino acid was removed by treatment with pyroglutamate aminopeptidase prior to protein sequencing by incubating 6 nmol of cytochrome c_2 in 75 m*M* phosphate buffer pH 7.0, 15 m*M* DTT and 3 units of pyroglutamate aminopeptidase at 310 K for 5 h. The cytochrome c_2 was separated from the enzyme by use of a microconcentrator (Amicon) with a 30 kDa cutoff membrane.

2.3. Protein characterization

The precise molecular weight of the purified cytochrome c_2 was determined using matrix-assisted laser desorption/ionization time-of-flight mass spectrometry (Vestec Lasertec Research). A matrix solution was prepared using sinapinic (3,5-dimethoxy 4-hydroxycinnamic) acid as a saturated solution in 0.1% trifluoroacetic acid containing 33% acetonitrile. The matrix solution was mixed with an equal volume of 50 µ*M* cytochrome c_2 and 1 µl aliquots were dried on stainless-steel pins for measurement. Measurements were calibrated using horse heart cytochrome with a molecular weight of 12 361 Da. Optical absorption measurements were performed using a Cary 5 spectrophotometer (Varian). Fully reduced and oxidized samples were prepared using 10 m*M* sodium ascorbate and 10 m*M* potassium ferricyanide, respectively. Electron transfer from the cytochrome c_2 to the bacterial reaction center was measured by monitoring the absorption changes at 550 nm arising from the introduction of an actinic light from a 1000 W tungsten source (Oriel).

2.4. Crystallization

Crystallization was carried out using the sitting-drop vapor-diffusion method at 277 K. Initially, crystals were obtained by mixing a protein solution at a concentration of 10 mg ml^{-1} with an equal volume of reservoir solution containing 100 m*M* sodium acetate pH 4.6 and 8% polyethylene glycol 4000. Although these crystals diffracted to high resolution, they were not suitable for diffraction experiments because of disorder. A second crystal form was obtained by mixing equal volumes of protein solution at a concentration of 20 mg ml^{-1} with reservoir solution consisting of 10% polyethylene glycol 6000 and 0.1 *M* phosphate buffer pH 7. Crystals generally

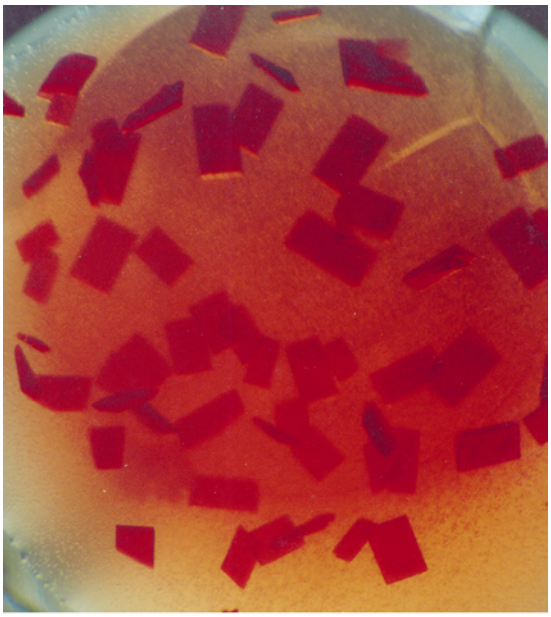

(*a*)

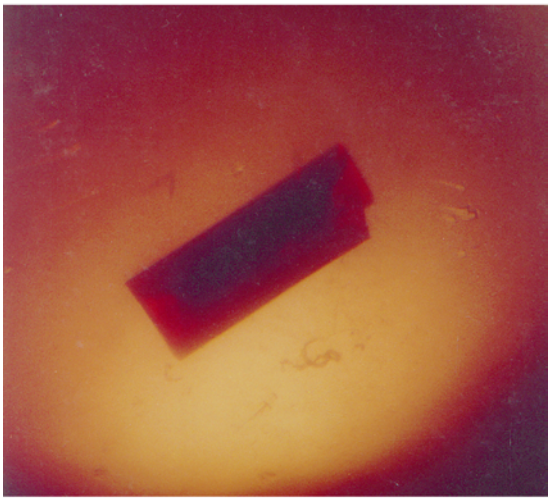

(*b*)

Figure 1
(*a*) Crystals grown in 10% polyethylene glycol 6000 and 0.1 *M* phosphate buffer pH 7 at 277 K after two weeks. The drop is approximately 5 mm wide and the crystals have a maximal length of 0.5 mm. (*b*) Crystals grown in one week by macroseeding. These crystals are larger in size, with a maximal length of 1.5 mm, and diffract to a higher resolution limit.

Table 1
Data-collection statistics.

Values in parentheses are for the outer shell, with a resolution range of 1.76–1.70 Å.

	Native	K_2PtCl_4
Resolution (Å)	20–1.7	20–1.7
Unit-cell parameters (Å)		
a	29.7	29.7
b	59.9	59.9
c	65.4	65.2
No. of observations	223519	89804
Unique reflections ($F > 2\sigma$)	13248 (1169)	13067 (1261)
Completeness (%)	98.6 (88.4)	97.5 (94.8)
Average $I/\sigma(I)$	2986 (149)	1398 (51)
R_{merge} (%)	7.0 (32)	9.3 (61)

grew to dimensions of 0.5 × 0.2 × 0.1 mm in two weeks, with a color typical of reduced cytochrome. Larger crystals with dimensions of 1.5 × 0.5 × 0.5 mm could be grown in one week by macroseeding (Fig. 1). For the macroseeding, an equilibrated protein solution was obtained by preparing the protein and reservoir solutions as described above for crystallization and allowing the solutions to equilibrate undisturbed for 1 d. After 1 d, the cover slip was removed and one or two small crystals that had been previously grown and soaked in serial dilutions of the reservoir solution were transferred to the equilibrated protein solution. The cover slip was then replaced and the crystals were allowed to grow without further manipulation.

For preparation of heavy-metal derivatives, the cytochrome crystals were initially transferred to a solution containing 10% polyethylene glycol 6000 and 0.1 *M* HEPES pH 7. After 2 d, the crystals were transferred to the same solution with the appropriate heavy metal added. The time of soaking in each metal was varied from 3 d to several weeks. The best derivatized form was obtained by soaking the cytochrome crystals as described above with 1 m*M* K_2PtCl_4 for three weeks.

2.5. Data collection

Diffraction data were collected from crystals mounted in glass capillaries at room temperature using a Rigaku R-AXIS IIC image-plate detector mounted on a Rigaku RU-200HB copper rotating-anode X-ray generator. The data were processed and scaled using *DENZO* and *SCALEPACK* (Otwinowski & Minor, 1997). All data sets were characterized by a high level of completeness, high resolution (1.7 Å), low R_{merge} values and high redundancy (Table 1). The data sets from individual crystals were incomplete owing to decay of the crystals during measurement. To obtain more complete data with 98.6% of all possible reflections, data from three single crystals were merged together. This increased the R_{merge} from an average of 4.0% for the individual data sets to 7.0%.

2.6. Phasing and refinement

Anomalous scattering from the Fe atom in the heme group was used for phase determination as previously described (Baker *et al.*, 1995). The Fe-atom position was obtained from a Patterson map calculated using the observed anomalous differences as coefficients with the program *XtalView* (McRee, 1999). Harker sections assuming a $P2_12_12_1$ space group revealed a single clear peak in each of the three 0.5 planes. Each of these peaks was approximately 10σ above background and three times greater than any other peaks. The program *xHercules* produced a maximum correlation value of 0.82 with $u = 0.119$, $v = 0.410$ and $w = 0.006$ (in reduced cell units) that was identified as arising from the Fe atom. The Fe-atom anomalous scattering was also identified using the program *CNS* (Brunger *et al.*, 1998) from the correlation coefficient for the best solution, which was 0.49 using the f2f2 target for refinement with a combined reciprocal-space and direct-space search method (Grosse-Kunstleve & Brunger, 1999). The calculated site position had the coordinates $x = 3.54$, $y = 5.38$ and $z = 0.40$, which is in agreement with the peaks found in Patterson maps. Using *CNS*, protein phases were calculated with 2 Å resolution data and phases were improved by solvent flattening. The calculated electron-density maps clearly showed a protein region and some secondary-structure elements. The maps revealed only one molecule within the asymmetric unit, as was expected based upon the Matthews coefficient of 2.1 and the corresponding solvent fraction of 41% (Matthews, 1968).

The structure of the cytochrome c_2 from *Rhodospirillum rubrum* (Salemme *et al.*, 1973; Bhatia, 1981) was used as a molecular-replacement model. The primary structures of these two cytochromes are similar except for the presence of a six-amino-acid residue insertion in the sequence of *R. centenum* relative to that of *Rhodospirillum rubrum* (Samyn *et al.*, 1998). Although a clear solution to the rotation function was obtained, no correct solution for the translation function was obtained. Using the experimental phases calculated from anomalous scattering, we repeated the molecular replacement using *CNS* (Adams *et al.*, 1999). The translation function had a clear solution with a monitor value of 0.256, compared with a mean value of 0.149 and a packing value of 0.51. An initial round of rigid-body refinement using *CNS* gave an R_{cryst} of 44.2% and an R_{free} of 46.2% for data to 2 Å resolution.

Electron-density maps calculated using the experimental anomalous scattering phase and the molecular-replacement solution gave a high-quality map. The Fe-atom position in the model structure was located in the same position as found by anomalous scattering. The backbone trace and secondary structure were clearly evident and the amino-acid sequence from *R. centenum* was substituted into the model without including the six-amino-acid insertion using the program *O* (Jones *et al.*, 1991). After a combined simulated-annealing and least-squares refinement, the model gave an R_{cryst} of 32.3% and an R_{free} factor of 36.7% for data to 2 Å resolution.

To improve the phases, several derivative data sets were collected. Patterson maps calculated from the K_2PtCl_4 derivative show only one major binding site (Table 1). Using *CNS*, the best solution correlation coefficient was 0.58 using the f2f2 target for refinement by a combined reciprocal-space and direct-space search method. The calculated site coordinates

were $x = 9.9$, $y = 3.9$, $z = 12.3$ and this site is located next to Met16 at position $x = 10.3$, $y = 2.4$, $z = 11.0$. The derivative phases were combined with those obtained from the anomalous scattering and molecular replacement using *CNS*. Cycles of structure refinement using least-squares and simulated annealing with the program *CNS* were combined with manual model building with *O*. The program *PROCHECK* (Laskowski *et al.*, 1993) was used to check the stereochemical and geometrical outliers in the final structure.

3. Results

3.1. Protein characterization

The purified protein was identified as a cytochrome c_2 based upon a number of properties. Peaks in the optical absorption spectrum at 412, 521 and 552 nm are characteristic of hemes (Moore & Pettigrew, 1990). The protein spectrum did not change in the presence of ascorbate, indicating that the sample was reduced. Under oxidizing conditions arising from the addition of ferricyanide, the 521 and 552 nm bands descreased in amplitude forming a broad unresolved band and the 412 nm band increased slightly in amplitude and shifted to a peak maximum of 417 nm. The crystals grown from these protein solutions were also reduced, as shown by the optical spectrum of the protein obtained after washing and dissolving the crystals.

The molecular weight was precisely determined to be 13 632 kDa by laser mass spectrometry, which is in agreement with previous measurements (Samyn *et al.*, 1998). When both the cytochrome and the bacterial reaction center were present in solution, the 552 nm band rapidly decreased when an actinic light was incident, demonstrating the ability of the cytochrome to serve as a secondary electron donor to the bacterial reaction center.

The N-terminus region of the protein was found to be initially blocked, but treatment using pyroglutamate aminopeptidase allowed the following sequence to be determined: pEDGDPAKGEAVFKKCMACHRV, where pE is pyroglutamate. This sequence has the C*XX*CH motif characteristic of heme-binding sites and matches identically the amino-acid sequence (Samyn *et al.*, 1998). The sequence and the molecular weight identify the protein as the iso-2 or acidic isozyme of cytochrome c_2 from *R. centenum* (Samyn *et al.*, 1998).

3.2. Structural model

The model of the cytochrome c_2 has a type I cytochrome fold (Fig. 2). The structure has six α-helices formed by residues 4–15, 50–59, 64–72, 74–86, 88–93 and 104–119. An unusual feature of the structure is the long α-helix formed by residues 74–86. Other cytochromes have only a short α-helix in this region. The longer helix in *R. centenum* arises from the presence of the six amino-acid residues not found in other cytochrome sequences. The heme is coordinated by Cys15 and Cys18, which form the thioether linkages to the heme group; His19 with Met98 form the extraplanar heme ligands (Fig. 2).

Table 2
Refinement statistics.

Values in parentheses are for the outer shell, with a resolution range of 1.76–1.70 Å.

Resolution range (Å)	20–1.7
R_{cryst} for 10556 working reflections (%)	19.2 (24.9)
R_{free} for 1079 test reflections (%)	21.0 (28.9)
Protein atoms	892
Solvent molecules	90
Deviations from ideal geometry	
Bond lengths (Å)	0.0055
Bond angles (°)	1.33
Ramachandran plot quality	
% in most favorable regions	89.8
% in additional allowed regions	9.2
% in disallowed regions	0
Average *B* values (Å^2)	
Protein	22.3
Solvent and side chains	26.8

The final model agrees well with measured structure factors, as the R_{cryst} is 19.4% and the R_{free} is 21.0% (Table 2). The temperature-factor values range from 10 to 72 Å^2 and the mean *B*-factor value is 23.7 Å^2. All amino-acid side chains fit the electron density well except for residues Asp24 and Glu90. Asp24 is placed in a solvent-exposed loop at the surface of the protein that is partially disordered. Glu90 is also located on the surface and forms a salt bridge with Lys26 from a symmetry-related protein in the crystal. Most of the lysine residues have poor density at the end of the side chain because of multiple conformations, although Lys26 does have density at the N^{ε} position, presumably as a result of the salt bridge with Glu90 stabilizing the side-chain position. Based upon the Ramachandran plot, the geometry of the model was excellent, with only one residue, Leu28, being out of the preferred zones. This residue is next to a proline residue in a classical reversed γ-turn in which the amido group of Leu28 forms a hydrogen bond with the carbonyl group of Gly30. This region, including the distorted geometry, is conserved among cytochromes (Sogabe & Miki, 1995; Louie & Brayer, 1990; Benning *et al.*, 1991, 1994, 1996) and is postulated to play an important role in orienting the protein backbone with respect to the heme group and in controlling ligand–metal interactions (Zhao *et al.*, 2000; Othman *et al.*, 1997). The geometry is also slightly distorted for Lys74, which is located between the two α-helices formed by residues 64–72 and 74–86. This residue is part of a type II β-turn that is conserved, with the distorted geometry, among cytochromes.

4. Discussion

The structure of cytochrome c_2 from *R. centenum* has been determined using X-ray diffraction at a resolution limit of 1.7 Å. The model has the unusual features of a long α-helix formed by residues 74–86 and a limited number of surface lysine residues. The implications of these features for the

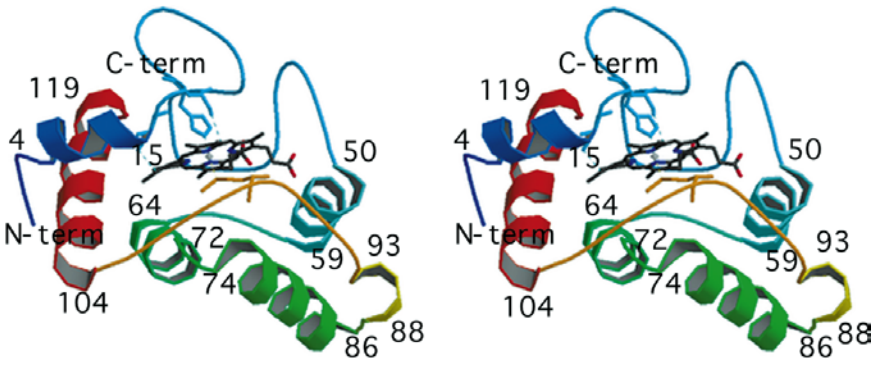

Figure 2
Stereo diagram of the three-dimensional structure of cytochrome c_2 from *R. centenum* in ribbon format. The residues at the beginning and end of each α-helix are indicated, as are the N- and C-termini. The heme prosthetic group and heme-binding residues Cys15, Cys18, His19 and Met98 are shown. Figures were drawn using the programs *XtalView* (McRee, 1999), *MOLSCRIPT* (Kraulis, 1991) and *RASTER3D* (Merritt & Bacon, 1997).

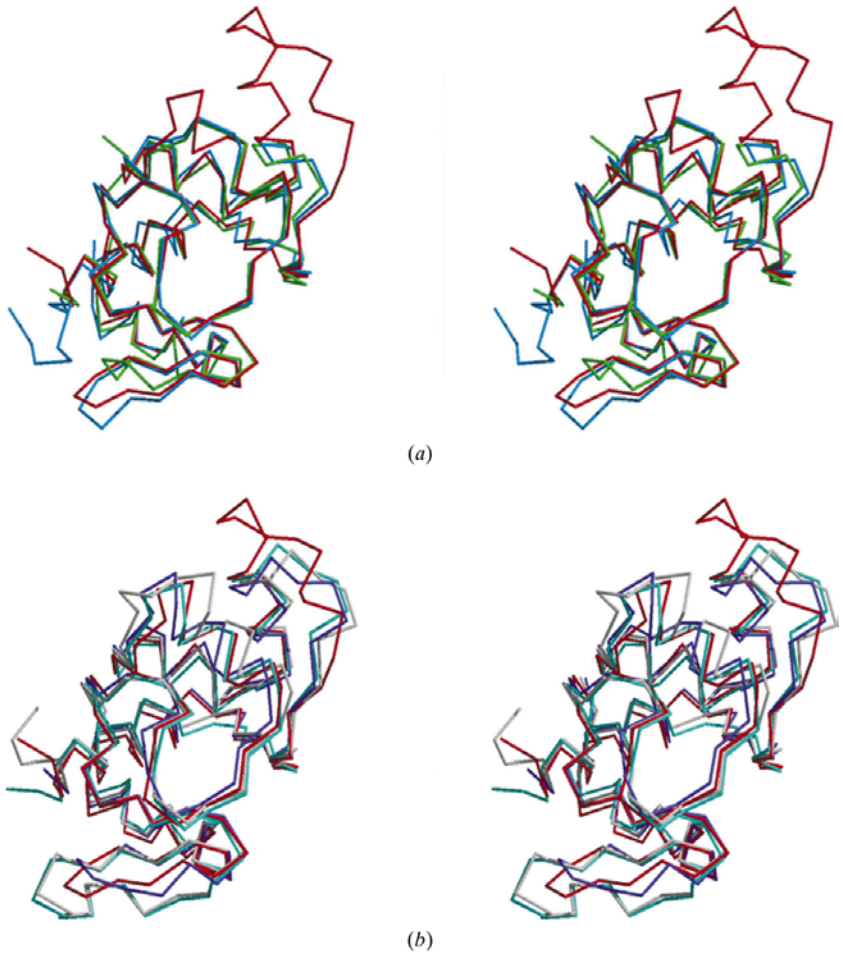

Figure 3
Comparison of cytochrome c_2 from *R. centenum* (red) with other cytochromes. (*a*) Superposition with bacterial eukaryotic type cytochromes from *Rhodopseudomonas viridis* (blue; PDB code 1co6) and *Rhodopseudomonas globiformis* (green; PDB code 1hro). (*b*) Superposition with longer chain cytochromes from *Rhodobacter sphaeroides* (pink; PDB code 1cxc), *Rhodobacter capsulatus* (pale blue; PDB code 1c2r) and *Rhodospirillum rubrum* (purple; PDB code 2c2c).

properties of cytochrome c_2, including its ability to serve as a secondary electron donor to the reaction center, are discussed below.

4.1. Comparison of the cytochrome c_2 from *R. centenum* to other cytochromes c_2

Based upon their amino-acid sequences and comparison with eukaryotic cytochromes, bacterial cytochromes c_2 can be grouped into two classes (Moore & Pettigrew, 1990). One class has a polypeptide chain of the same length as that of eukaryotic cytochromes (less than 110 residues) and a second class has longer chains, with at least two insertions of three and eight residues. Most bacterial sequences belong to the second group, with only the sequences from *Rhodopseudomonas viridis* and *Rhodopseudomonas globiformis* being comparable to eukaryotic sequences. The cytochrome from *R. centenum* can be assigned to the second class according to its length, but it also has features of the first class (Fig. 3). For example, the cytochrome c_2 from *R. centenum* has a short hairpin turn between residues 18 and 28 as seen in the eukaryotic type sequences. The *R. centenum* cytochrome also has a large loop formed by residues 84–91 that resembles the corresponding region of the second class rather than the eukaryotic cytochromes. As found in other bacterial cytochromes, the N-terminal α-helix is distorted to form a thioether bond from Cys15 to the heme group, as seen for the cytochrome c_2 in *Rhodopseudomonas viridis* (Sogabe & Miki, 1995). This distortion does not appear in eukaryotic cytochromes *c*, which have one additional amino-acid residue. The N-terminal α-helix is in close contact with the C-terminal α-helix, resulting in Phe12 being in van der Waals contact with Phe108 and Tyr114. The orientation of their aromatic rings are arranged such that favorable positive and negative dipole interactions could take place between the π-electron cloud and the partially positive H atom of the planar ring.

All *c*-type cytochromes show the motif C*XX*CH, where the cysteine side chains form thioether likages with the heme group and the histidine side chain is coordinated to the heme iron. The distances from the heme iron to the coordinating His19 N^{ε} and to Met98 S^{δ} are 2.1 and 2.3 Å, respectively. The angle formed by this bond and the porphyrin ring plane is 82.7°. This deviation from being precisely perpendicular is also evident in other cytochrome structures. The heme group is also slightly bent, with pyrrole

rings B and C, which are involved in thioether linkages, showing a higher deviation with respect to the porphyrin-ring planarity, as found in other cytochromes c_2 (Sogabe & Miki, 1995).

The surrounding environment establishes the oxidation/reduction potential of the heme group, with the cytochrome c_2 from *R. centenum* having a potential of 293 mV (Samyn *et al.*, 1998). The heme pocket is highly hydrophobic, with surrounding aromatic amino-acid residues including Tyr49, Tyr71, Phe47, Phe100 and Trp63. Two buried water molecules are located in the heme-binding pocket and are bound by a hydrogen-bond network (Fig. 4). These water molecules are well ordered as shown by their low *B*-factor values and they are in the same position as the conserved water molecules found in eukaryotic cytochrome *c* proteins. One water molecule, located near the heme propionate and Thr96, has been shown to move closer to the heme iron of eukaryotic cytochromes as they are oxidized (Takano & Dickerson, 1980, 1981*a*,*b*). The second water molecule interacts with the other heme propionate and it is within hydrogen-bonding distance of Tyr49, Gln40 and Arg39. These water molecules have been proposed to play a role in the redox potential of the heme group by stabilizing the oxidized state (Bushnell *et al.*, 1990). The potential has also been proposed to be influenced by an interaction between a conserved tyrosine (residue 71 in *R. centenum*) and the methionine coordinating the heme iron (residue 98 in *R. centenum*) (Takano & Dickerson, 1981). For example, the cytochrome from *Rhodopseudomonas globiformis* has an unusually high midpoint potential of 450 mV owing to various features including a weak interaction between the corresponding tyrosine and methionine (Benning *et al.*, 1996). In the cytochrome from *R. centenum*, the distance between the phenolic O atom of the tyrosine and the S atom of the coordinating methionine is large at 3.2 Å. This distance in *R. centenum* is very comparable to the corresponding distance in *Rhodopseudomonas globiformis*, which would suggest comparable potentials for the two cytochromes. However, the potential is much lower in *R. centenum* and hence the large distance is inconsistent with a significant role of this interaction in establishing the redox potential.

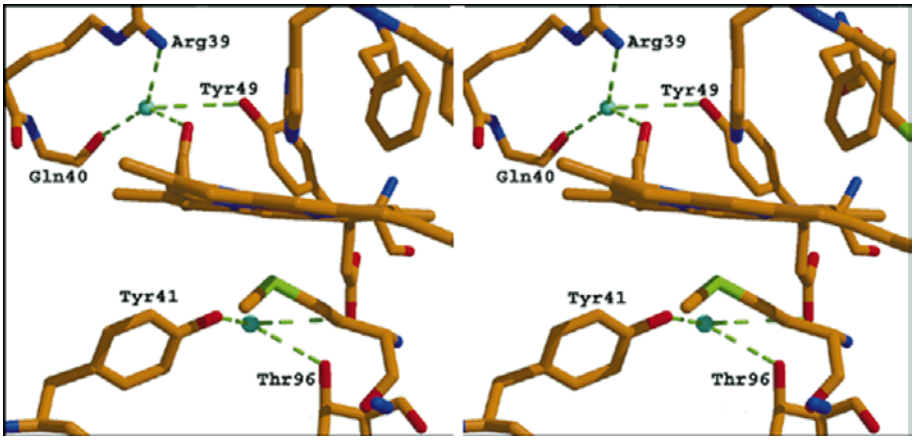

Figure 4
Stereo diagram of the heme pocket with the conserved water molecules. Residues to which water molecules form hydrogen bonds are shown. The water molecules shown have low temperature factors of 17.0 and 19.2 Å^2; they are placed in roughly the same position as other eukaryotic and prokaryotic cytochromes *c*.

In addition to the cytochrome c_2 described in this report, a second

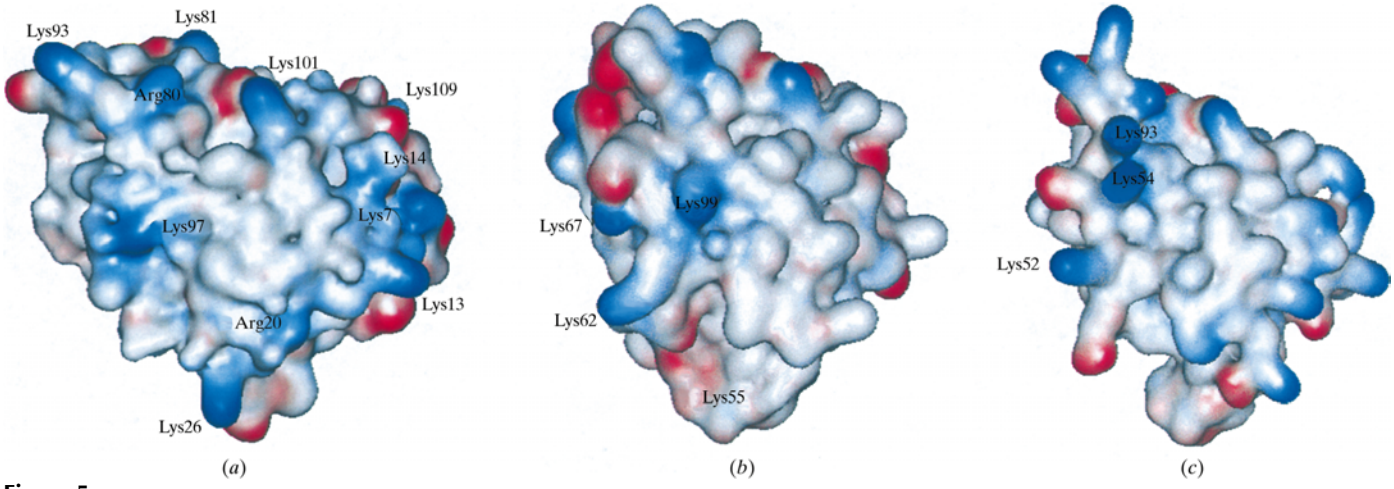

Figure 5
Electrostatic surfaces from the frontside of cytochrome c_2 from (*a*) *R. centenum*, (*b*) *Rhodobacter sphaeroides* and (*c*) *Rhodobacter capsulatus*. Negatively charged residues are shown in red and positively charged residues are shown in blue. In *R. centenum*, three distinct regions that probably contribute to the reaction-center binding are evident on the surface. The central region has Lys97 contributing a charge and is otherwise largely neutral. At the upper right, there is a positive region formed by residues Lys81, Lys93, Lys101 and Arg80. This region is unique to the cytochrome c_2 from *R. centenum*. At the lower left, a positively charged region is formed by residues Lys7, Lys13 and Lys109.

isozyme is expressed in *R. centenum* (Samyn *et al.*, 1998). Of the 119 residues of the cytochrome, all but 18 are identical between the two proteins. The majority of the non-conserved residues are located on the surface of the structure, with five being in the segment formed by residues 84–91 (Fig. 2). Six of the non-conserved residues are located in the heme pocket. Nine of the substitutions are relatively conservative and may result in minor functional changes, such as a midpoint potential of 316 mV for the second isozyme compared with the 293 mV potential determined for the cytochrome described in this report. Since none of these differences involve residues identified as critical for function, the two isozymes can probably serve comparable functions.

4.2. Implications for cytochrome c_2 binding to the reaction center

During photosynthesis, cytochrome c_2 binds to the reaction center, transfers an electron to the photo-oxidized bacteriochlorophyll dimer and then is released into the periplasmic region. Different molecular models of cytochrome c_2 binding to the periplasmic side of reaction centers have been proposed (Allen *et al.*, 1987; Tiede *et al.*, 1993; Adir *et al.*, 1996; Axelrod *et al.*, 1994). Central to all of the proposed models is the importance of electrostatic interactions involving lysine side chains on the cytochrome surface and carboxylate groups on the reaction center in establishing the structure of the complex, in accordance with the observation that the binding is strongly dependent upon the ionic strength. In addition to the reaction center from *R. centenum*, the cytochrome c_2 from *R. centenum* can transfer an electron to reaction centers from *Rhodobacter sphaeroides* and *Rhodobacter capsulatus* (Lin *et al.*, 1994; Wang *et al.*, 1994). While cytochrome c_2 from *Rhodobacter sphaeroides* and *Rhodobacter capsulatus* can bind tightly to reaction centers from both species, the cytochrome c_2 from *R. centenum* does not bind to reaction centers from *Rhodobacter sphaeroides* and forms a complex with but binds 20-fold more weakly to reaction centers from *Rhodobacter capsulatus*.

The distribution of the surface charges on the cytochrome c_2 from *R. centenum* should differ from those of other cytochromes and be related to the observed differences in binding. The cytochromes c_2 from *Rhodobacter sphaeroides* and *Rhodobacter capsulatus* have several lysines in the central region of the surface that have been proposed as playing a critical role in binding (Allen *et al.*, 1987; Tiede *et al.*, 1993; Adir *et al.*, 1996). In contrast, in this region of the surface in the cytochrome c_2 from *R. centenum* there is only one Lys, residue 97, that could contribute to electrostatic binding (Fig. 5). The diminished binding affinity of the cytochrome c_2 from *R. centenum* probably reflects the lack of these lysine residues. Two regions of the surface of the cytochrome c_2 from *R. centenum* have pronounced contributions of positive charge (Fig. 5). A cluster of charges in the upper region is formed by Lys81, Lys93, Lys101 and Arg80. This region is unique to the cytochrome c_2 from *R. centenum* as it is formed by the long extended α-helix of the cytochrome. Several Lys residues are found in the homologous region in *Rhodobacter capsulatus*, although the spatial distribution is significantly different to that found in *R. centenum*. The presence of this positive region may lead to a difference in residues forming the binding region for the cytochrome c_2 from *R. centenum* compared with other cytochromes. The other region is at the lower edge of the surface, with contributions from residues Lys7, Lys13 and Lys109. While the corresponding region of cytochrome c_2 from *Rhodobacter capsulatus* also has several positive charges, this region is largely neutral for the cytochrome c_2 from *Rhodobacter sphaeroides*. The ability of the cytochrome c_2 from *R. centenum* to bind to the reaction center from *Rhodobacter capsulatus* but not *Rhodobacter sphaeroides* suggests an involvement of this region in the formation of this complex.

We thank X. Li for the protein purification and D. Brune for the protein sequencing and mass spectrometry. This work was supported by grant No. 1999–01753 from the USDA.

References

Adams, P. D., Pannu, N. S., Read, R. J. & Brunger, A. T. (1999). *Acta Cryst.* D**55**, 181–190.
Adir, N., Axelrod, H. L., Beroza, P., Isaacson, R. A., Rongey, S. H., Okamura, M. Y. & Feher, G. (1996). *Biochemistry*, **35**, 2535–2547.
Allen, J. P., Feher, G., Yeates, T. O., Komiya, H. & Rees, D. C. (1987). *Proc. Natl Acad. Sci. USA*, **84**, 5730–5734.
Axelrod, H. L., Feher, G., Allen, J. P., Chirino, A. J., Day, M. W., Hsu, B. T. & Rees, D. C. (1994). *Acta Cryst.* D**50**, 596–602.
Baker, E. N., Anderson, B. F., Dobbs, A. J. & Dodson, E. J. (1995). *Acta Cryst.* D**51**, 282–289.
Bartsch, R. G. (1978). *The Photosynthetic Bacteria*, edited by R. K. Clayton & W. R. Sistrom, pp. 249–279. New York: Plenum Press.
Benning, M. M., Meyer, T. E. & Holden, H. M. (1994). *Arch. Biochem. Biophys.* **310**, 460–466.
Benning, M. M., Meyer, T. E. & Holden, H. M. (1996). *Arch. Biochem. Biophys.* **333**, 338–348.
Benning, M. M., Wesenberg, G., Caffrey, M. S., Bartsch, R. G., Meyer, T. E., Cusanovich, M. A., Rayment, I. & Holden, H. M. (1991). *J. Mol. Biol.* **220**, 673–685.
Bhatia, G. E. (1981). PhD thesis, University of California, San Diego, USA.
Brunger, A. T., Adams, P. D., Clore, G. M., DeLano, W. L., Gros, P., Grosse-Kunstleve, R. W., Jiang, J. S., Kuszewski, J., Nilges, M., Pannu, N. S., Read, R. J., Rice, L. M., Simonson, T. & Warren, G. L. (1998). *Acta Cryst.* D**54**, 905–921.
Bushnell, G. W., Louie, G. V. & Brayer, G. D. (1990). *J. Mol. Biol.* **214**, 585–595.
Grosse-Kunstleve, R. W. & Brunger, A. T. (1999). *Acta Cryst.* D**55**, 1568–1577.
Jones, T. A., Zou, J. Y., Cowan, S. W. & Kjeldgaard, M. (1991). *Acta Cryst.* A**47**, 110–119.
Kraulis, P. J. (1991). *J. Appl. Cryst.* **24**, 946–950.
Laskowski, R. A., MacArthur, M. W., Moss, D. S. & Thornton, J. M. (1993). *J. Appl. Cryst.* **26**, 283–291.
Lin, X., Williams, J. C., Allen, J. P. & Mathis, P. (1994). *Biochemistry*, **33**, 13517–13523.
Louie, G. V. & Brayer, G. D. (1990). *J. Mol. Biol.* **214**, 527–555.
McRee, D. E. (1999). *J. Struct. Biol.* **125**, 156–165.
Matthews, B. W. (1968). *J. Mol. Biol.* **33**, 491–497.
Merritt, E. A. & Bacon, D. J. (1997). *Methods Enzymol.* **277**, 505–524.

Meyer, T. E. & Donohue, T. J. (1995). *Anoxygenic Photosynthetic Bacteria*, edited by R. E. Blankenship, M. T. Madigan & C. E. Bauer, pp. 725–745. Dordrecht: Kluwer Academic Publishers.
Moore, G. R. & Pettigrew, G. W. (1990). *Cytochromes c: Evolutionary, Structural and Physicochemical Aspects.* Berlin: Springer-Verlag.
Othman, S., Fitch, J., Cusanovich, M. A. & Desbois, A. (1997). *Biochemistry*, **36**, 5499–5508.
Otwinowski, Z. & Minor, W. (1997). *Methods Enzymol.* **276**, 307–326.
Salemme, F. R., Kraut, J. & Kamen, M. D. (1973). *J. Biol. Chem.* **248**, 7701–7716.
Samyn, B., Fitch, J., Meyer, T. E., Cusanovich, M. A. & Van Beeumen, J. J. (1998). *Biochim. Biophys. Acta*, **1384**, 345–355.
Sogabe, S. & Miki, K. (1995). *J. Mol. Biol.* **252**, 235–247.
Takano, T. & Dickerson, R. E. (1980). *Proc. Natl Acad. Sci. USA*, **77**, 6371–6375.
Takano, T. & Dickerson, R. E. (1981*a*). *J. Mol. Biol.* **153**, 79–94.
Takano, T. & Dickerson, R. E. (1981*b*). *J. Mol. Biol.* **153**, 95–115.
Tiede, D. M., Vashishta, A. C. & Gunner, M. R. (1993). *Biochemistry*, **32**, 4515–4531.
Wang, S., Li, X., Williams, J. C., Allen, J. P. & Mathis, P. (1994). *Biochemistry*, **33**, 8306–8312.
Yildiz, F. H., Gest, H. & Bauer, C. E. (1991). *J. Bacteriol.* **173**, 5502–5506.
Zhao, D. Z., Hutton, H. M., Meyer, T. E., Walker, F. A., MacKenzie, N. E. & Cusanovich, M. A. (2000). *Biochemistry*, **39**, 4053–4061.